

Investigating α clustering on the surface of ^{120}Sn via the $(p, p\alpha)$ reaction, and the validity of the factorization approximation

Kazuki Yoshida,^{*} Kosho Minomo, and Kazuyuki Ogata*Research Center for Nuclear Physics (RCNP), Osaka University, Ibaraki 567-0047, Japan*

(Received 2 March 2016; revised manuscript received 15 July 2016; published 10 October 2016)

The $^{120}\text{Sn}(p, p\alpha)^{116}\text{Cd}$ reaction at 392 MeV is investigated with the distorted wave impulse approximation (DWIA) framework. We show that this reaction is very peripheral, mainly because of the strong absorption of α by the reaction residue ^{116}Cd , and the α clustering on the nuclear surface can be probed clearly. We investigate also the validity of the so-called factorization approximation that has frequently been used so far. It is shown that the kinematics of α in the nuclear interior region is significantly affected by the distortion of ^{116}Cd , but it has no effect on the reaction observables because of the strong absorption in that region.

DOI: [10.1103/PhysRevC.94.044604](https://doi.org/10.1103/PhysRevC.94.044604)

I. INTRODUCTION

Nuclear clustering has been one of the main subjects in nuclear physics; for a recent review, see Ref. [1]. As a new topic, α clustering on the surface of heavy nuclei, Sn isotopes, is theoretically predicted in Ref. [2]. This result itself is interesting and important because it has been believed that α clustering is developed mainly in light nuclei, although some indication for α clustering in ^{40}Ca and ^{44}Ti was discussed [3]. Furthermore, the result gives a significant impact on the nuclear equation of state [2].

As emphasized in Ref. [1], however, one should keep it in mind that a large spectroscopic factor of α does not necessarily indicate the α clustering, because of the *duality* of the mean-field-type structure and the cluster structure [4]. On the other hand, the localization of α in the nuclear surface region is direct evidence of the α clustering in a nucleus. In this view, the α transfer reaction, $(^6\text{Li}, d)$ in particular, has been utilized for investigating the α clustering. Very recently, a three-body reaction model with a microscopic cluster wave function was applied to the $^{16}\text{O}(^6\text{Li}, d)^{20}\text{Ne}$ reaction and the transfer cross section was shown to be sensitive to the α distribution on the nuclear surface of ^{20}Ne [5].

In the present study, as an alternative way to the α transfer reaction, we consider the proton-induced α knockout reaction on ^{120}Sn , and investigate how clearly it can probe the α distribution in the surface region of ^{120}Sn , i.e., the α clustering of ^{120}Sn . We adopt the distorted wave impulse approximation (DWIA) framework to describe the $(p, p\alpha)$ reaction; DWIA has successfully been used in the analysis of various nucleon knockout [6–11] and α knockout [12–18] experiments. In many preceding studies, however, the so-called factorization approximation, which factors out the nucleon-nucleon (NN) transition amplitude in the evaluation of the total transition matrix element of the knockout process, has been adopted. In this paper we explicitly examine the validity of the factorization approximation by means of the local semiclassical approximation (LSCA) [19,20] to the distorted waves. It was argued in Ref. [6] that the factorization approximation

becomes questionable when the distortion effect is large. It is thus important to examine its validity for the α knockout process for a heavy nucleus, in which the distortion on α by the reaction residue is expected to be very strong.

In Sec. II we describe the DWIA formalism for the $(p, p\alpha)$ reaction, introducing the LSCA that is a key prescription for discussing the accuracy of the factorization approximation. In Sec. III first we show the comparison between the present calculation and the experimental data. Next we discuss the validity of the factorization approximation in the $^{120}\text{Sn}(p, p\alpha)^{116}\text{Cd}$ reaction at 392 MeV. We then show that the $^{120}\text{Sn}(p, p\alpha)^{116}\text{Cd}$ reaction probes the α distribution in the surface region with high selectivity. The dependence of these findings on the α wave function is also discussed. Finally, a summary is given in Sec. IV.

II. FORMALISM

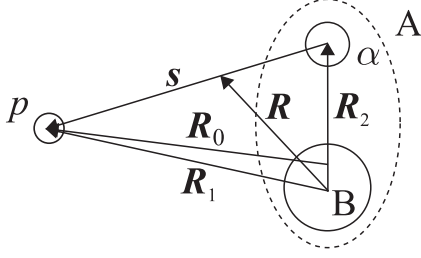
We consider the $A(p, p\alpha)B$ reaction in normal kinematics in the DWIA framework. The incoming proton in the initial channel is labeled as particle 0, and the outgoing proton and α are particles 1 and 2, respectively. A (B) denotes the target (residual) nucleus. \mathbf{K}_i and Ω_i ($i = 0, 1, 2$) represent the momentum and its solid angle, respectively, and E_i (T_i) is the total (kinetic) energy of particle i . All quantities with and without superscript L indicate that they are evaluated in the laboratory (L) and center-of-mass (c.m.) frame, respectively.

The transition amplitude in the DWIA formalism is given by

$$T_{\mathbf{K}_0 \mathbf{K}_1 \mathbf{K}_2}^{nljm} = \langle \chi_{1, \mathbf{K}_1}^{(-)}(\mathbf{R}_1) \chi_{2, \mathbf{K}_2}^{(-)}(\mathbf{R}_2) | t_{p\alpha}(s) | \chi_{0, \mathbf{K}_0}^{(+)}(\mathbf{R}_0) \varphi_{\alpha}^{nljm}(\mathbf{R}_2) \rangle, \quad (1)$$

where χ_0 , χ_1 , and χ_2 are the scattering wave functions of the p -A, p -B, and α -B systems, respectively, $t_{p\alpha}$ is the transition interaction between p and α , and φ_{α}^{nljm} is the α -cluster wave function. n , l , j , and m are, respectively, the principal quantum number, the orbital angular momentum, the total angular momentum, and its third component of α in the nucleus A. The superscripts (+) and (−) specify the outgoing and incoming boundary conditions on χ_i , respectively. The definition of the coordinates is given in Fig. 1.

* yoshidak@rcnp.osaka-u.ac.jp

FIG. 1. Coordinates of A($p, p\alpha$)B reaction.

By using

$$\mathbf{R} = \frac{1}{A_\alpha + 1} \mathbf{R}_1 + \frac{A_\alpha}{A_\alpha + 1} \mathbf{R}_2, \quad (2)$$

$$s = \mathbf{R}_1 - \mathbf{R}_2, \quad (3)$$

\mathbf{R}_i are written by

$$\mathbf{R}_0 = \mathbf{R}_1 - \frac{A_\alpha}{A} \mathbf{R}_2 = \left(1 - \frac{A_\alpha}{A}\right) \mathbf{R} + \alpha_0 \frac{A_\alpha}{A_\alpha + 1} s, \quad (4)$$

$$\mathbf{R}_1 = \mathbf{R} + \frac{A_\alpha}{A_\alpha + 1} s, \quad (5)$$

$$\mathbf{R}_2 = \mathbf{R} - \frac{1}{A_\alpha + 1} s, \quad (6)$$

where $A_\alpha = 4$ and $\alpha_0 = (A + 1)/A$ with A being the mass number of A. We make the LSCA [19,20] that describes the propagation of the scattering wave for a short distance ΔR by a plane wave, i.e.,

$$\chi_{i, \mathbf{K}_i}(\mathbf{R} + \Delta \mathbf{R}) \approx \chi_{i, \mathbf{K}_i}(\mathbf{R}) e^{i \mathbf{K}_i(\mathbf{R}) \cdot \Delta \mathbf{R}}. \quad (7)$$

The norm of the local momentum $\mathbf{K}_i(\mathbf{R})$ is given by

$$|\mathbf{K}_i(\mathbf{R})| = \text{Re}[\mathbf{K}_i^C(\mathbf{R})], \quad (8)$$

where the complex momentum $\mathbf{K}_i^C(\mathbf{R})$ is determined so as to satisfy the local energy conservation:

$$\frac{(\hbar \mathbf{K}_i)^2}{2\mu_i} = \frac{[\hbar \mathbf{K}_i^C(\mathbf{R})]^2}{2\mu_i} + U_i(\mathbf{R}) \quad (9)$$

with μ_i and $U_i(\mathbf{R})$ being the reduced mass of the scattering particles and the distorting potential for particle i , respectively. The direction of $\mathbf{K}_i(\mathbf{R})$ is taken to be parallel to the flux of $\chi_{i, \mathbf{K}_i}(\mathbf{R})$. The validity of the LSCA is discussed in Sec. III C.

Equation (1) is then reduced to

$$T_{K_0 K_1 K_2}^{nljm} \approx \int d\mathbf{R} F_{K_0 K_1 K_2}(\mathbf{R}) \varphi_\alpha^{nljm}(\mathbf{R}) \tilde{t}_{p\alpha}[\kappa'(\mathbf{R}), \kappa(\mathbf{R})], \quad (10)$$

where $F_{K_0 K_1 K_2}(\mathbf{R})$ and $\tilde{t}_{p\alpha}[\kappa'(\mathbf{R}), \kappa(\mathbf{R})]$ are defined by

$$F_{K_0 K_1 K_2}(\mathbf{R}) \equiv \chi_{1, K_1}^{*(-)}(\mathbf{R}) \chi_{2, K_2}^{*(-)}(\mathbf{R}) \chi_{0, K_0}^{(+)}(\mathbf{R}) \times e^{-i \mathbf{K}_0(\mathbf{R}) \cdot \mathbf{R} A_\alpha / A}, \quad (11)$$

$$\tilde{t}_{p\alpha}[\kappa'(\mathbf{R}), \kappa(\mathbf{R})] \equiv \int ds e^{-i \kappa'(\mathbf{R}) \cdot s} t_{p\alpha}(s) e^{i \kappa(\mathbf{R}) \cdot s}. \quad (12)$$

Here, $\kappa(\mathbf{R})$ [$\kappa'(\mathbf{R})$] is the p - α relative momentum in the initial (final) channel:

$$\kappa(\mathbf{R}) \equiv \alpha_0 \frac{A_\alpha}{A_\alpha + 1} \mathbf{K}_0(\mathbf{R}) - \frac{1}{A_\alpha + 1} \mathbf{K}_\alpha(\mathbf{R}), \quad (13)$$

$$\kappa'(\mathbf{R}) \equiv \frac{A_\alpha}{A_\alpha + 1} \mathbf{K}_1(\mathbf{R}) - \frac{1}{A_\alpha + 1} \mathbf{K}_2(\mathbf{R}). \quad (14)$$

$\mathbf{K}_\alpha(\mathbf{R})$ is determined by the momentum conservation of the p - α system:

$$\mathbf{K}_\alpha(\mathbf{R}) = \mathbf{K}_1(\mathbf{R}) + \mathbf{K}_2(\mathbf{R}) - \alpha_0 \mathbf{K}_0(\mathbf{R}). \quad (15)$$

In taking the squared modulus of Eq. (10), we make the on-the-energy-shell (on-shell) approximation to $\tilde{t}_{p\alpha}$:

$$\frac{\mu_{p\alpha}^2}{(2\pi \hbar^2)^2} |\tilde{t}_{p\alpha}[\kappa'(\mathbf{R}), \kappa(\mathbf{R})]|^2 \approx \frac{d\sigma_{p\alpha}}{d\Omega_{p\alpha}} [\theta_{p\alpha}(\mathbf{R}), E_{p\alpha}(\mathbf{R})], \quad (16)$$

where $\theta_{p\alpha}(\mathbf{R})$ is the angle between $\kappa(\mathbf{R})$ and $\kappa'(\mathbf{R})$, i.e., the local p - α scattering angle, and $E_{p\alpha}(\mathbf{R})$ is the local scattering energy defined by

$$E_{p\alpha}(\mathbf{R}) = \frac{\hbar^2 [\kappa'(\mathbf{R})]^2}{2\mu_{p\alpha}}. \quad (17)$$

In Eqs. (16) and (17) $\mu_{p\alpha}$ is the reduced mass of the p - α system.

With the LSCA and the on-shell approximation, the triple differential cross section (TDX) of the ($p, p\alpha$) reaction is given by

$$\frac{d^3\sigma}{dE_1^L d\Omega_1^L d\Omega_2^L} = S_\alpha F_{\text{kin}} C_0 \sum_m |\tilde{T}_{K_0 K_1 K_2}^{nljm}|^2, \quad (18)$$

where S_α is the spectroscopic factor of the α cluster and the kinematical factor F_{kin} is defined by

$$F_{\text{kin}} \equiv J_L \frac{K_1 K_2 E_1 E_2}{\hbar^4 c^4} \left[1 + \frac{E_2}{E_B} + \frac{E_2}{E_B} \frac{\mathbf{K}_1 \cdot \mathbf{K}_2}{K_2^2} \right]^{-1} \quad (19)$$

with J_L being the Jacobian from the c.m. frame to the L frame, and

$$C_0 = \frac{E_0}{(hc)^2 K_0} \frac{1}{(2\ell + 1)} \frac{\hbar^4}{(2\pi)^3 \mu_{p\alpha}^2}. \quad (20)$$

The reduced transition amplitude is given by

$$\tilde{T}_{K_0 K_1 K_2}^{nljm} = \int d\mathbf{R} \sqrt{\frac{d\sigma_{p\alpha}}{d\Omega_{p\alpha}} (\theta_{p\alpha}(\mathbf{R}), E_{p\alpha}(\mathbf{R}))} \times F_{K_0 K_1 K_2}(\mathbf{R}) \varphi_\alpha^{nljm}(\mathbf{R}). \quad (21)$$

In the preceding studies on knockout reactions [6–11], further simplification of $\tilde{T}_{K_0 K_1 K_2}^{nljm}$ was made by replacing $\mathbf{K}_i(\mathbf{R})$ with the asymptotic momentum \mathbf{K}_i . We then obtain

$$\frac{d^3\sigma}{dE_1^L d\Omega_1^L d\Omega_2^L} \rightarrow F_{\text{kin}} C_0 \frac{d\sigma_{p\alpha}}{d\Omega_{p\alpha}} (\theta_{p\alpha}, E_{p\alpha}) \times \sum_m \left| \int d\mathbf{R} F_{K_0 K_1 K_2}(\mathbf{R}) \varphi_\alpha^{nljm}(\mathbf{R}) \right|^2, \quad (22)$$

where $\theta_{p\alpha}$ and $E_{p\alpha}$ are given in the same way as for $\theta_{p\alpha}(\mathbf{R})$ and $E_{p\alpha}(\mathbf{R})$, respectively, but with using the asymptotic p - α relative momenta:

$$\kappa \equiv \alpha_0 \frac{A_\alpha}{A_\alpha + 1} \mathbf{K}_0 - \frac{1}{A_\alpha + 1} \mathbf{K}_\alpha, \quad (23)$$

$$\kappa' \equiv \frac{A_\alpha}{A_\alpha + 1} \mathbf{K}_1 - \frac{1}{A_\alpha + 1} \mathbf{K}_2. \quad (24)$$

This prescription is called the factorization approximation. One sees that this approximation is equivalent to use the asymptotic momentum \mathbf{K}_i instead of the local momentum $\mathbf{K}_i(\mathbf{R})$ in Eq. (7), i.e.,

$$\chi_{i,\mathbf{K}_i}(\mathbf{R} + \Delta\mathbf{R}) \approx \chi_{i,\mathbf{K}_i}(\mathbf{R}) e^{\mathbf{K}_i \cdot \Delta\mathbf{R}}, \quad (25)$$

which we call the asymptotic momentum approximation (AMA). Therefore the accuracy of the factorization approximation can be judged, in principle, by that of the AMA.

III. RESULTS AND DISCUSSION

A. Numerical inputs

For the bound-state wave function φ_α^{nljm} , we assume that the α particle is bound in the $4S$ orbit in a Woods-Saxon potential $V(R) = V_0/[1 + \exp\{(R - r_0 A^{1/3})/a_0\}]$ with $r_0 = 1.27$ fm and $a_0 = 0.67$ fm. The depth of the potential V_0 is adjusted so as to reproduce the α separation energy of ^{120}Sn , 4.81 MeV. In the calculation shown below, the α spectroscopic factor S_α for ^{120}Sn is taken to be 0.022 [21]. It should be noted that the purpose of the present study is not to determine S_α but to understand the property of the $(p, p\alpha)$ knockout reaction and to examine the reliability of DWIA with the factorization approximation.

One of the most important ingredients of the present DWIA is the p - α differential cross section $d\sigma_{p\alpha}/d\Omega_{p\alpha}$ that determines the transition strength of the $(p, p\alpha)$ process. Because $d\Omega_{p\alpha}$ for various scattering energies and angles are needed, we adopt the microscopic single folding model [22] with implementing the phenomenological nuclear density of α and the Melbourne NN g -matrix interaction [23]. As shown in Fig. 2, with no free parameter, the calculated $d\sigma_{p\alpha}/d\Omega_{p\alpha}$ agrees very well with the experimental data [24,25] at 297 and 500 MeV.

As for the distorting potential for α in the final channel, for consistency, we employ the double-folding model [26] using the same ingredients as used in the p - α calculation; we use the nuclear density of ^{116}Cd calculated by the Hartree-Fock method in the same way as Ref. [27]. It is known that to phenomenologically determine a low-energy scattering potential of α is quite difficult because of the discrete ambiguities [28,29]. In fact, there have been many attempts [30–32] to microscopically determine an α potential with the double-folding model approach. It should be noted, however, that in the present study we evaluate both the real and imaginary parts of the α potential with no free adjustable parameter, in contrast to those preceding studies. For the distorting potential of proton in the initial and final channels, we use the EDAD1 parameter set of the Dirac phenomenology [33]. The Coulomb terms of the distorting

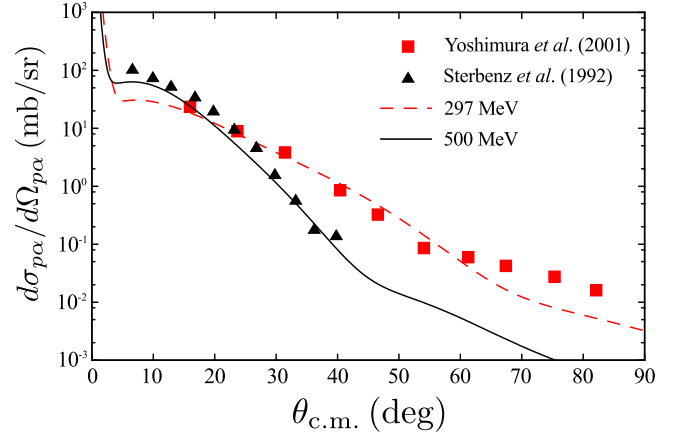


FIG. 2. Comparison between the $d\sigma_{p\alpha}/d\Omega_{p\alpha}$ calculated by the single-folding model calculation and the experimental data [24,25] at 297 and 500 MeV.

potentials are constructed by assuming that the target (residual) nucleus is a uniformly charged sphere with the radius of $r_0 A^{1/3}$ ($r_0 B^{1/3}$).

The effect of the nonlocality of the proton and α distorting potentials is taken into account by multiplying the scattering waves by the Perey factor [34] $F_P(R) = [1 - \mu\beta^2/(2\hbar^2)U(R)]^{-1/2}$, where μ is the reduced mass between the two scattering particles. The range of nonlocality β for p (α) is taken to be 0.85 fm (0.2 fm) [35].

We take the following kinematical condition on the $^{120}\text{Sn}(p, p\alpha)^{116}\text{Cd}$ reaction at 392 MeV; the Madison convention is adopted. The kinetic energy of particle 1 is fixed at 328 MeV and its emission angle is set to $(\theta_1, \phi_1) = (43.2^\circ, 0^\circ)$. As for particle 2, ϕ_2 is fixed at 180° and θ_2 is varied around 61° ; the kinetic energy T_2 changes around 59 MeV and $\theta_{p\alpha} \sim 56^\circ$, $E_{p\alpha} \sim 385$ MeV, accordingly [36]. We always adopt the relativistic kinematics for all the scattering particles in this study.

B. Test of the present calculation

We test the present model calculation by comparing the calculated result of the energy sharing cross section, which is a TDX with fixed $d\Omega_1^L$ and $d\Omega_2^L$, as a function of T_1 for $^{66}\text{Zn}(p, p\alpha)^{62}\text{Ni}$ reaction with measured experimental data [12]; the incident energy is 101.5 MeV. The present result and the experimental data are shown in Fig. 3. The EDAD parameter set are used for the distorting potential of p - ^{66}Zn and p - ^{62}Ni , and the double-folding model is adopted for α - ^{62}Ni , in the same way as in III A. According to Ref. [12], we assume that the α particle is bound in the $6S$ state in a Woods-Saxon potential with $r_0 = 1.30$ fm and $a_0 = 0.67$ fm, and the depth of the potential V_0 is adjusted so as to reproduce the α separation energy 4.58 MeV.

One can see that the present calculation well reproduces the observed energy-sharing cross section; the deduced α spectroscopic factor is 0.84, which is sizably larger than the value 0.42 obtained in the previous study [12]. It should be noted, however, that the double-folding model for the

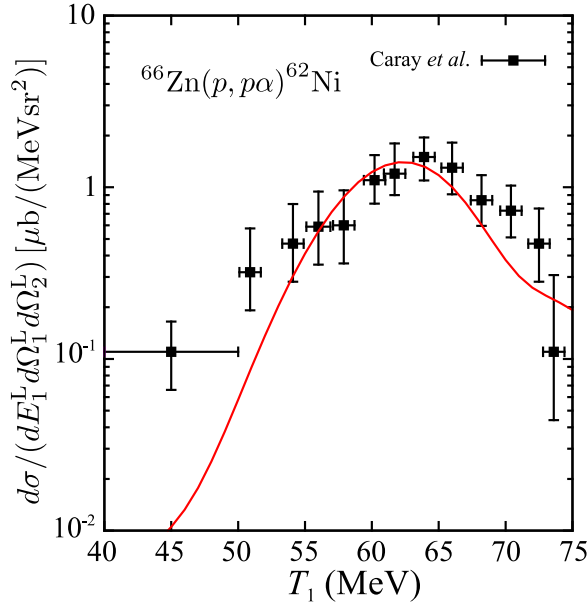


FIG. 3. Calculated energy sharing cross section of ${}^{66}\text{Zn}(p, p\alpha){}^{62}\text{Ni}$ reaction at 101.5 MeV. The experimental data are from Ref. [12].

distorting potential of α - ${}^{62}\text{Ni}$ will have some ambiguities due to the relatively low scattering energy of $T_2 \sim 30$ MeV. Furthermore, the calculated result in Ref. [12] showed quite large ambiguities ($\sim 50\%$) of the deduced α spectroscopic factors due to the α - ${}^{62}\text{Ni}$ potential. Considering these facts, it can be concluded that the present result is consistent with the experimental data and its analysis.

C. Validity of the LSCA and the AMA

The validity of the LSCA for the scattering of nucleon has been examined in Refs. [20,27] and it was concluded that at energies higher than about 50 MeV, the LSCA works for the propagation within 1.5 fm. Furthermore, at those energies the AMA is found to work at almost the same level as the LSCA [27]. Considering the aforementioned kinematical condition on particles 0 and 1, one may conclude that for proton both the LSCA and the AMA are valid in the description of the ${}^{120}\text{Sn}(p, p\alpha){}^{116}\text{Cd}$ reaction. On the other hand, such a validation for particle 2, the knocked out α particle, has not been done before.

In Fig. 4 we show the validity of the LSCA and the AMA for $\chi_{2, K_2}^{*(-)}$ with $(\theta_2, \phi_2) = (61^\circ, 180^\circ)$, which corresponds to the quasifree condition; i.e., the residual nucleus ${}^{116}\text{Cd}$ is at rest in the L frame. Figures 4(a) and 4(b) correspond to the propagation from $\mathbf{R}_a \equiv (7 \text{ fm}, 61^\circ, 180^\circ)$ and $\mathbf{R}_b \equiv (7 \text{ fm}, 29^\circ, 0^\circ)$, respectively, in the spherical coordinate representation. In each panel the solid, dashed, and dotted lines show, respectively, the real part of the exact wave function, that with the LSCA and that with the AMA. Since \mathbf{R}_a (\mathbf{R}_b) corresponds to the foreside (left side) of ${}^{116}\text{Cd}$ with respect to the outgoing α , the distortion effect on α at \mathbf{R}_a (\mathbf{R}_b) is weak (strong).

With weak distortion, as shown in Fig. 4(a), both approximations work well within about 0.5 fm of the propagation. It

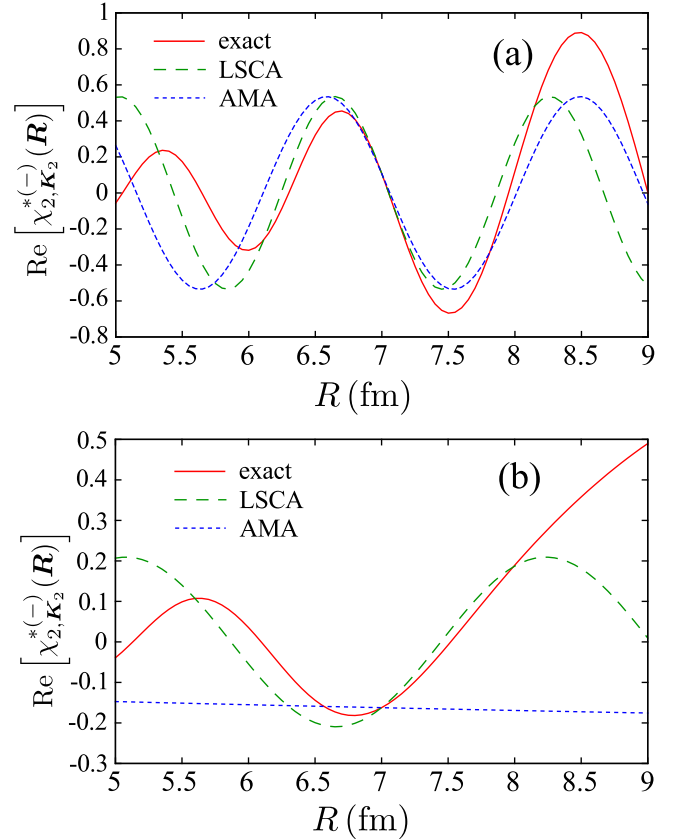


FIG. 4. The test of the LSCA and the AMA. The real part of $\chi_{2, K_2}^{*(-)}$ with no approximation (solid line), with the LSCA (dashed line), and with the AMA (dotted line) are plotted. In Figs. 4(a) and 4(b), the propagation from $(7 \text{ fm}, 61^\circ, 180^\circ)$ and $(7 \text{ fm}, 29^\circ, 0^\circ)$ are investigated, respectively; $(\theta_2, \phi_2) = (61^\circ, 180^\circ)$ is chosen for the kinematics of the α particle.

should be noted that, with considering the range of the p - α interaction of about 2 fm and the constant $1/(A_\alpha + 1) = 1/5$ in front of s in Eq. (6), the LSCA and the AMA are required to be valid for the propagation of about 0.4 fm. The two approximations are thus validated for the propagation from \mathbf{R}_a . In the case of the strong distortion, as shown in Fig. 4(b) and suggested in Ref. [6], the AMA cannot describe the behavior of the exact scattering wave function; since the radial direction from \mathbf{R}_b is almost orthogonal to the direction of the asymptotic momentum \mathbf{K}_2 , the dotted line is almost constant, whereas the solid line shows clear variation. On the other hand, the LSCA reproduces well the exact solution at almost the same level as in the case of weak distortion. Thus, one sees that the kinematics of α at \mathbf{R}_b is significantly changed from that in the asymptotic region by the distorting potential of ${}^{116}\text{Cd}$; this kinematical change is well traced by using the LSCA, i.e., the local momentum of the α particle.

Therefore one can conclude that the LSCA works for the α scattering wave function that is strongly distorted, whereas the AMA not. This may cast doubt on the use of the factorization approximation for the $(p, p\alpha)$ reaction investigated in the present study. In the following subsections we discuss this in view of the TDX.

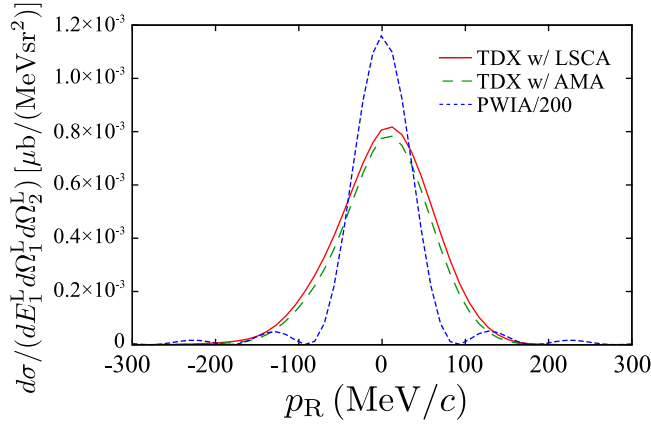


FIG. 5. TDX as a function of the recoil momentum. The solid (dashed) line corresponds to the calculation without (with) the factorization approximation. The TDX calculated with the PWIA divided by 200 is also shown by the dotted line.

D. TDX for the $^{120}\text{Sn}(p, p\alpha)^{116}\text{Cd}$ reaction at 392 MeV

The calculated TDX is shown in Fig. 5 as a function of the recoil momentum p_R defined by

$$p_R = \hbar K_B^L \frac{K_{Bz}^L}{|K_{Bz}^L|}. \quad (26)$$

The solid and dashed lines represent the results without and with the factorization approximation, respectively. One sees from the good agreement between the solid and dashed lines that the factorization approximation, or equivalently, the AMA, affects the TDX very little, although the AMA for α is shown to be invalid around R_b . This is due to the strong absorption of α in that region as shown in Sec. III E.

The dotted line in Fig. 5 represents the result of the plane wave impulse approximation (PWIA) calculation divided by 200. The renormalization factor 1/200 shows the strong absorption mainly caused by the α - ^{116}Cd distorting potential. In the PWIA, the TDX is essentially proportional to the absolute square of the Fourier transform of the α distribution φ_α^{nljm} inside ^{120}Sn . Since we take a 4S state, the dashed line in Fig. 6 shown below, the TDX calculated with the PWIA shows an oscillation pattern accordingly. The shape of the TDX calculated with the DWIA is quite different from that with the PWIA. The widening of the width of the TDX caused by distortion suggests that, because of the uncertainty principle, only a limited region of φ_α^{nljm} is probed by the $(p, p\alpha)$ reaction, as shown in Sec. III E. It should be noted that the slight shift of the peak of the TDX with the DWIA from $p_R = 0$ is understood by the shift of the momentum of particles 2 due to the real part of the distorting potential [37].

E. Probed region of α in ^{120}Sn by the $(p, p\alpha)$ reaction

In Fig. 6, we show by the solid line the absolute value of the integrand on the right-hand side of Eq. (21) after integration

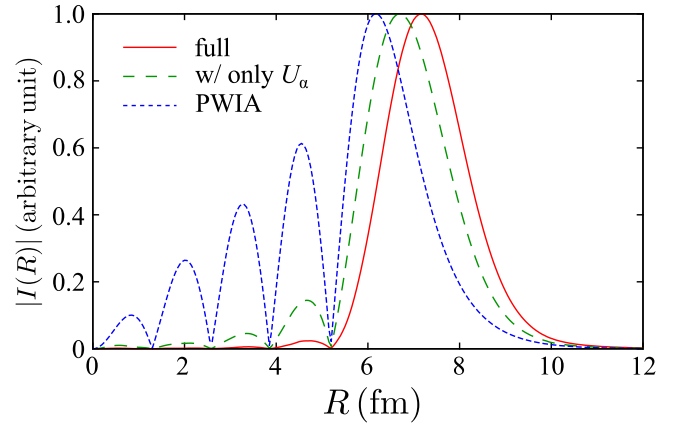


FIG. 6. $|I(R)|$ at $p_R = 0$ (solid line), the same but calculated with only the α - ^{116}Cd distorting potential U_α (dashed line), and the result with PWIA (dotted line). The results are normalized to unity at the peak position.

over the solid angle Ω of \mathbf{R} :

$$I(R) \equiv \int d\Omega R^2 \sqrt{\frac{d\sigma_{p\alpha}}{d\Omega_{p\alpha}}[\theta_{p\alpha}(\mathbf{R}), E_{p\alpha}(\mathbf{R})]} \times F_{K_0 K_1 K_2}(\mathbf{R}) \varphi_\alpha^{nljm}(\mathbf{R}); \quad (27)$$

the plotted result corresponds to $p_R = 0$, i.e., the quasifree condition. The dashed line shows $|I(R)|$ calculated with including only U_α , the distorting potential of the α - ^{116}Cd system in the final state, and the dotted line shows that with PWIA. Each line is normalized to unity at the peak position. One sees that the magnitude of $I(R)$ is strongly suppressed in the interior region, $R \lesssim 6$ fm, mainly because of the absorption due to the α - ^{116}Cd distorting potential. The slight shift of the peak position is due to the suppression in the interior region. It should be noted, however, that the product of the oscillating three distorted waves and a bound-state wave function can make nontrivial cancellation. This property also may contribute to the aforementioned suppression.

Furthermore, in Fig. 7 the TDXs calculated with changing the minimum value R_{\min} of the integration over R are shown; we take $R_{\min} = 0, 6, 6.5, 7,$ and 8 fm. It is found that the calculated TDX does not change for $R_{\min} = 0$ – 5.5 fm, and decreases drastically for $R_{\min} = 6$ – 8 fm. The slight increase of TDX with $R_{\min} = 6$ fm is due to the interference of the integrand. This result shows that the $(p, p\alpha)$ reaction on heavy nuclei probes the α -cluster wave function on the nuclear surface with high selectivity, as required for the reaction to be a good probe for α clustering. With this peripherality of the $(p, p\alpha)$ reaction, one can understand naturally the mechanism that makes the width of the TDX wider when the distortion is taken into account.

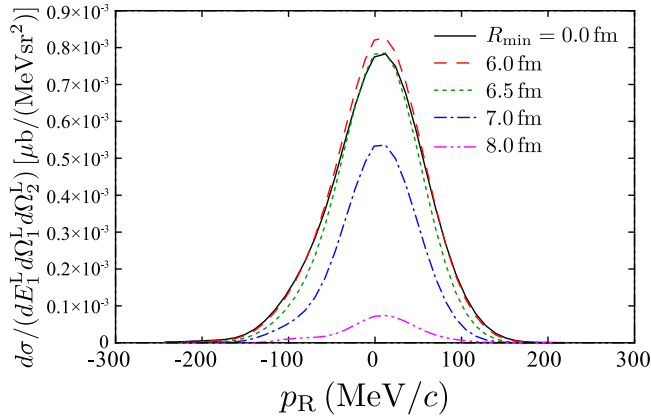


FIG. 7. Same as Fig. 5 but with changing R_{\min} . The solid, dashed, dotted, dot-dashed, and two-dot-dashed lines correspond to $R_{\min} = 0, 6, 6.5, 7,$ and 8 fm, respectively.

For more detailed analysis, the absolute value of the integrand on the right-hand side of Eq. (21)

$$J(\mathbf{R}) \equiv \sqrt{\frac{d\sigma_{p\alpha}}{d\Omega_{p\alpha}}[\theta_{p\alpha}(\mathbf{R}), E_{p\alpha}(\mathbf{R})] F_{K_0 K_1 K_2}(\mathbf{R}) \varphi_{\alpha}^{nljm}(\mathbf{R})} \quad (28)$$

on the z - x plane for $y = 0, 1, 3, 5, 6,$ and 7 fm are shown in Figs. 8(a)–8(f). For $y = 0, 1,$ and 3 fm, it is clearly seen that the amplitude is located in the foreside region with $R = 6$ – 9 fm, where $\chi_{2, K_2}^{(-)}(\mathbf{R})$ is not absorbed and $\varphi_{\alpha}(\mathbf{R})$ has a finite amplitude. For $y \geq 5$ fm, the localization of the amplitude becomes rather vague, because the absorption property of

$\chi_{2, K_2}^{(-)}(\mathbf{R})$ does not strongly depend on z and x for such values of y . Nevertheless, one may see that the main part of $|J(\mathbf{R})|$ exist in the foreside region. Figures 8(a)–8(f) therefore show that the $(p, p\alpha)$ reaction has selectivity not only in the radius but also the direction of the target nucleus.

It is found that the peak at the rear side on $y = 0$ plane, around $\mathbf{R} = (6$ – 8 fm, $120^\circ, 0^\circ)$ in Fig. 8(a) comes from the focus of $\chi_{2, K_2}^{*(-)}$ due to the attraction of the distorting potential and the increase in $d\sigma_{p\alpha}/d\Omega_{p\alpha}$ caused by that. It should be noted that this rear-side peak exists only at around $y = 0$ as shown in Fig. 8, and makes no major contribution to the TDX. In fact, it is found that about 90% of the TDX comes from the $x < 0$ region. This means that the possible interference between the amplitudes in the fore-side and rear-side regions is very small, which realizes an intuitive picture that the $(p, p\alpha)$ reaction of our interest takes place in a limited region of space. These features support idea that the AMA is valid for the calculation of the TDX.

F. Discussion of α -cluster wave function

Since a very naive model for φ_{α} is adopted in the present study, it is important to see the φ_{α} dependence of the findings discussed above. It is obvious that the validity of the LSCA itself has nothing to do with φ_{α} . Thus, we discuss the φ_{α} dependence of the TDX as well as effect of the AMA on that. In Fig. 9 the solid (dotted) line shows the TDX calculated with φ_{α} with increasing (decreasing) the range parameter r_0 by 10%, $r_0 = 1.40$ (1.14) fm; these results are obtained by using the LSCA. The dashed line is the same as the solid line in Fig. 5. One can see that the 10% difference of r_0 changes

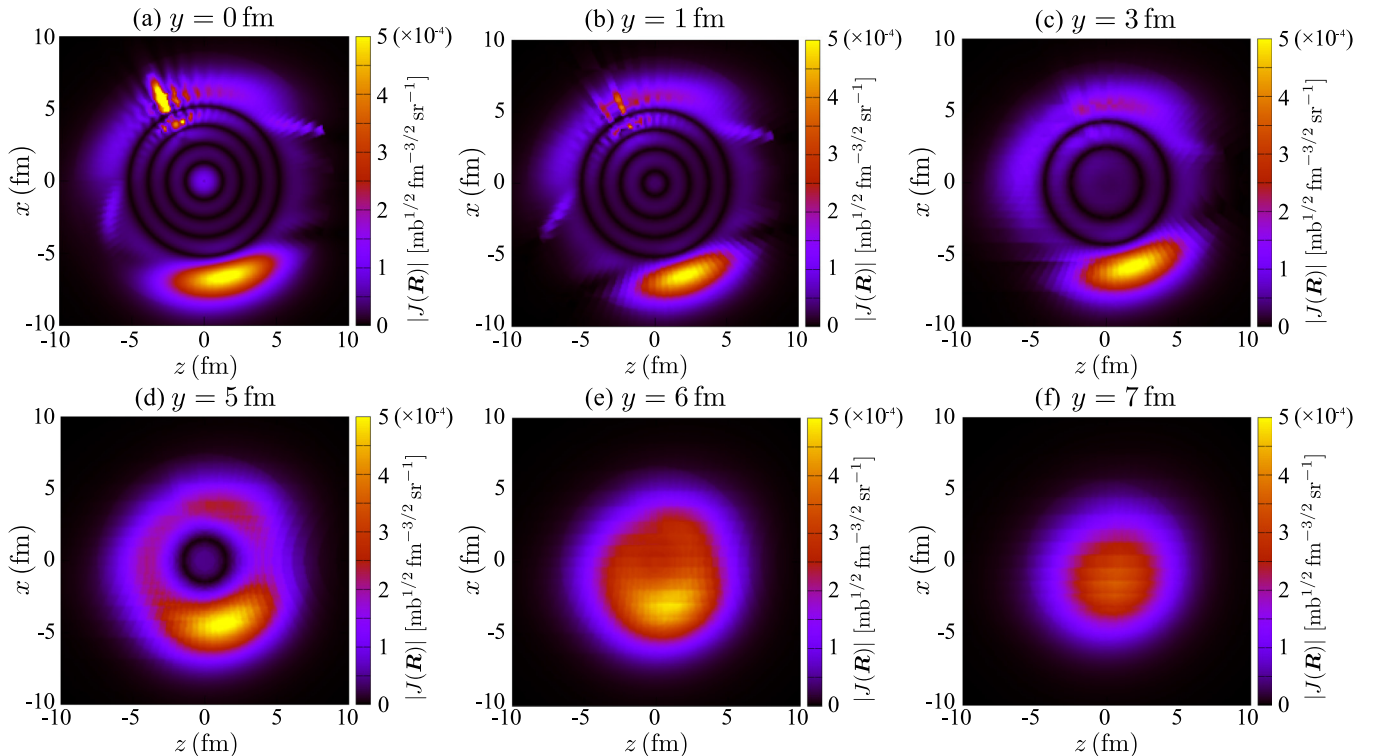


FIG. 8. $|J(\mathbf{R})|$ on the z - x plane for $y = 0, 1, 3, 5, 6,$ and 7 fm. The kinematical condition is the same as in Fig. 6.

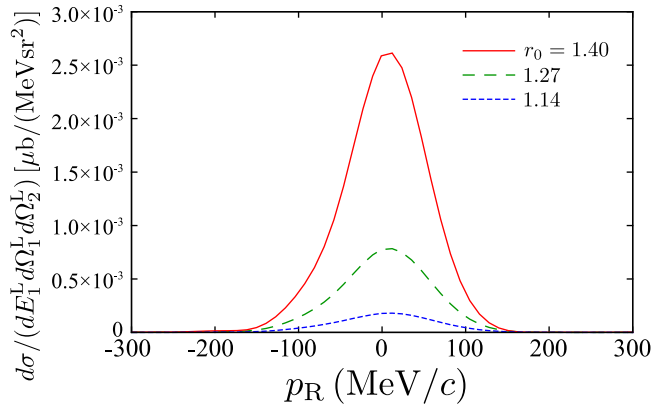


FIG. 9. The TDXs with different r_0 . The solid (dotted) line is the TDX with $r_0 = 1.40$ (1.14) fm. The dashed line is the same as in Fig. 5 for comparison.

the magnitude of the TDX significantly, i.e., by about a factor of three difference. This is also understood by the absorption in the interior region. Since only the surface region contributes to the TDX, small extension of φ_α to the exterior region changes the magnitude of TDX drastically. It is found that the TDX at $p_R = 0$ calculated with the AMA differs from that with the LSCA by only 6% at most. Furthermore, the qualitative features shown in Figs. 7 and 8 turned out to be independent of r_0 .

IV. SUMMARY

We have examined the $^{120}\text{Sn}(p, p\alpha)^{116}\text{Cd}$ reaction at 392 MeV in the DWIA framework. To show the validity of the DWIA model, we have demonstrated that it reproduces the observed energy sharing cross section data of $^{66}\text{Zn}(p, p\alpha)^{62}\text{Ni}$ at 101.5 MeV. It was clarified that the so-called factorization approximation adopted in many preceding studies is equivalent

to the AMA to the distorted waves, which is a further simplification of the LSCA. Although the AMA does not work for the propagation of α in the region where the nuclear deflection is significant, it does not affect the TDX because of the strong absorption in that region. In other words, the integrand of the transition matrix has a contribution only in the region where the AMA works well. As a result, the factorization approximation was verified for the calculation of the TDX of the $(p, p\alpha)$ reaction. It should be kept in mind, however, that the inaccuracy of the AMA may affect the TDX if a scattering particle feels a potential having a strong real part and a weak imaginary part; this can be realized, for instance, for nucleon scattering at lower energies. The strong absorption due to the α - ^{116}Cd distorting potential makes the $(p, p\alpha)$ reaction very peripheral, which allows one to clearly probe the α -clustering of nuclei. Furthermore, the $(p, p\alpha)$ reaction has high selectivity also in the direction of the target nucleus; only the fore-side region with respect to the emitting α with the radius of 6–9 fm is probed. It is also shown that the factorization approximation and the peripherality of the reaction are valid for different choices of φ_α , but the magnitude of TDXs are strongly dependent on them. This result suggests that it is essential to employ a reliable α -cluster wave function for the qualitative discussion.

Validation of the on-shell approximation to the p - α transition amplitude will be important for more reliable description of the knockout processes.

ACKNOWLEDGMENTS

The authors thank S. Kawase and T. Uesaka for fruitful discussions. The computation was carried out with the computer facilities at the Research Center for Nuclear Physics, Osaka University. This work was supported in part by Grants-in-Aid of the Japan Society for the Promotion of Science (Grants No. JP15J01392 and No. JP25400255) and by the ImPACT Program of the Council for Science, Technology and Innovation (Cabinet Office, Government of Japan).

-
- [1] H. Horiuchi, K. Ikeda, and K. Katō, *Prog. Theor. Phys. Suppl.* **192**, 1 (2012).
 - [2] S. Typel, *Phys. Rev. C* **89**, 064321 (2014).
 - [3] T. Yamaya, K. Katori, M. Fujiwara, S. Kato, and S. Ohkubo, *Prog. Theor. Phys. Suppl.* **132**, 73 (1998).
 - [4] B. F. Bayman and A. Bohr, *Nucl. Phys.* **9**, 596 (1958/59).
 - [5] T. Fukui, Y. Taniguchi, T. Suhara, Y. Kanada-En'yo, and K. Ogata, *Phys. Rev. C* **93**, 034606 (2016).
 - [6] C. Samanta, N. S. Chant, P. G. Roos, A. Nadasen, J. Wesick, and A. A. Cowley, *Phys. Rev. C* **34**, 1610 (1986).
 - [7] N. S. Chant and P. G. Roos, *Phys. Rev. C* **15**, 57 (1977).
 - [8] C. Samanta, N. S. Chant, P. G. Roos, A. Nadasen, and A. A. Cowley, *Phys. Rev. C* **35**, 333 (1987).
 - [9] G. Jacob and Th. A. J. Maris, *Rev. Mod. Phys.* **38**, 121 (1966).
 - [10] G. Jacob and Th. A. J. Maris, *Rev. Mod. Phys.* **45**, 6 (1973).
 - [11] P. Kitching, W. J. McDonald, Th. A. J. Maris, and C. A. Z. Vasconcelos, *Adv. Nucl. Phys.* **15**, 43 (1985).
 - [12] T. A. Carey, P. G. Roos, N. S. Chant, A. Nadasen, and H. L. Chen, *Phys. Rev. C* **29**, 1273 (1984).
 - [13] J. Mabilia, A. A. Cowley, S. V. Förtsch, E. Z. Buthelezi, R. Neveling, F. D. Smit, G. F. Steyn, and J. J. Van Zyl, *Phys. Rev. C* **79**, 054612 (2009).
 - [14] P. G. Roos, N. S. Chant, A. A. Cowley, D. A. Goldberg, H. D. Holmgren, and R. Woody III, *Phys. Rev. C* **15**, 69 (1977).
 - [15] A. Nadasen, N. S. Chant, P. G. Roos, T. A. Carey, R. Cowen, C. Samanta, and J. Wesick, *Phys. Rev. C* **22**, 1394 (1980).
 - [16] A. Nadasen, P. G. Roos, N. S. Chant, C. C. Chang, G. Ciangaru, H. F. Breuer, J. Wesick, and E. Norbeck, *Phys. Rev. C* **40**, 1130 (1989).
 - [17] C. W. Wang, P. G. Roos, N. S. Chant, G. Ciangaru, F. Khazaie, D. J. Mack, A. Nadasen, S. J. Mills, R. E. Warner, E. Norbeck, F. D. Becchetti, J. W. Janecke, and P. M. Lister, *Phys. Rev. C* **31**, 1662 (1985).

- [18] T. Yoshimura, A. Okihana, R. E. Warner, N. S. Chant, P. G. Roos, C. Samanta, S. Kakigi, N. Koori, M. Fujiwara, N. Matsuoka, K. Tamura, E. Kubo, and K. Ushiro, *Nucl. Phys. A* **641**, 3 (1988).
- [19] Y. L. Luo and M. Kawai, *Phys. Rev. C* **43**, 2367 (1991).
- [20] Y. Watanabe, R. Kuwata, Sun Weili, M. Higashi, H. Shinohara, M. Kohno, K. Ogata, and M. Kawai, *Phys. Rev. C* **59**, 2136 (1999).
- [21] J. Jänecke, F. D. Becchetti, and C. E. Thorn, *Nucl. Phys. A* **325**, 337 (1979).
- [22] M. Toyokawa, K. Minomo, and M. Yahiro, *Phys. Rev. C* **88**, 054602 (2013).
- [23] K. Amos, P. J. Dortmans, H. V. von Geramb, S. Karataglidis, and J. Raynal, *Adv. Nucl. Phys.* **25**, 276 (2000).
- [24] M. Yoshimura, M. Nakamura, H. Akimune, I. Daito, T. Inomata, M. Itoh, M. Kawabata, T. Noro, H. Sakaguchi, H. Takeda, A. Tamii, K. Yonehara, H. P. Yoshida, and M. Yosoi, *Phys. Rev. C* **63**, 034618 (2001).
- [25] S. M. Sterbenz, D. Dehnhard, M. K. Jones, S. K. Nanda, C. E. Parman, Y.-F. Yen, K. W. Jones, and C. L. Morris, *Phys. Rev. C* **45**, 2578 (1992).
- [26] K. Egashira, K. Minomo, M. Toyokawa, T. Matsumoto, and M. Yahiro, *Phys. Rev. C* **89**, 064611 (2014).
- [27] K. Minomo, K. Ogata, M. Kohno, Y. R. Shimizu, and M. Yahiro, *J. Phys. G* **37**, 085011 (2010).
- [28] M. Nolte, H. Machner, and J. Bojowald, *Phys. Rev. C* **36**, 1312 (1987).
- [29] *Proceedings of the 2nd Louvain Cracow Seminar on the Alpha Nucleus Interaction, Louvain-la-Neuve, 1978*, edited by G. Gregoire and K. Grotowski (Universite de Lourain-la-Neuve, 1978), and references therein.
- [30] S. Ohkubo and Y. Hirabayashi, *Phys. Rev. C* **70**, 041602(R) (2004).
- [31] D. C. Cuong, D. T. Khoa, and G. Colò, *Nucl. Phys. A* **836**, 11 (2010).
- [32] T. Furumoto and Y. Sakuragi, *Phys. Rev. C* **74**, 034606 (2006).
- [33] S. Hama, B. C. Clark, E. D. Cooper, H. S. Sherif, and R. L. Mercer, *Phys. Rev. C* **41**, 2737 (1990); E. D. Cooper, S. Hama, B. C. Clark, and R. L. Mercer, *ibid.* **47**, 297 (1993).
- [34] G. Perey and B. Buck, *Nucl. Phys.* **32**, 353 (1962).
- [35] TWOFNR, *User Manual*, <http://www.nucleartheory.net/NPG/codes/twofnr.pdf>.
- [36] T. Uesaka (private communication).
- [37] K. Ogata, K. Yoshida, and K. Minomo, *Phys. Rev. C* **92**, 034616 (2015).